International Journal of Global Warming

ISSN online: 1758-2091 - ISSN print: 1758-2083
https://www.inderscience.com/ijgw

Spatio-temporal dynamics of land use effects on surface temperature in a Mediterranean city: a case study

Pınar Zeğerek Altunbey, Sıla Balta

DOI: 10.1504/IJGW.2025.10068013

Article History:

Received:	09 May 2024
Last revised:	23 October 2024
Accepted:	24 October 2024
Published online:	10 January 2025

Spatio-temporal dynamics of land use effects on surface temperature in a Mediterranean city: a case study

Pınar Zeğerek Altunbey*

Department of Landscape Architecture,
Faculty of Architecture,
Nigde Omer Halisdemir University,
51240, Niğde, Türkiye
Email: zegerek.pinar@gmail.com
*Corresponding author

Sıla Balta

Department of Landscape Architecture,
Faculty of Fine Arts and Design,
Inonu University,
44280, Malatya, Türkiye
Email: silabalta00@gmail.com

Abstract: This research investigates the impact of LULC changes on LST in Antalya from 1984 to 2022. It also statistically analysed the effects of spectral indices such as NDVI and NDBI on LST. Antalya is experiencing a rapid land transformation with agricultural lands decreasing by 44.79% and natural lands by 72.16%, changing to artificial surfaces. Over this period, the maximum surface temperature value increased from 37.7°C in 1984 to 50.5°C in 2022. Therefore, the research highlights the consequences of transforming agricultural lands to urban areas, in Antalya, where tourism is dominant in land use change.

Keywords: land surface temperature; LST; Mediterranean; remote sensing; urban heat island; UHI; urbanisation.

Reference to this paper should be made as follows: Zeğerek Altunbey, P. and Balta, S. (2025) 'Spatio-temporal dynamics of land use effects on surface temperature in a Mediterranean city: a case study', *Int. J. Global Warming*, Vol. 35, No. 1, pp.33–50.

Biographical notes: Pınar Zeğerek Altunbey is currently a Research Assistant at Nigde Omer Halisdemir University, Faculty of Architecture, Department of Landscape Architecture. She took her MSc and PhD at Akdeniz University in Türkiye. Her research interests include landscape planning, urban green area planning, landscape design, GIS, and remote sensing, and landscape management.

Sıla Balta is currently a Research Assistant at Inonu University, Faculty of Fine Arts and Design, Department of Landscape Architecture. She took her MSc and PhD at Akdeniz University in Türkiye. Her research interests include landscape planning, urban planning, landscape design, GIS, and remote sensing.

1 Introduction

People are moving toward urbanisation due to social, economic, and environmental factors, leading to rapid landscape change and the establishment of urban environmental norms (Humbal et al., 2023; Oke et al., 2017). Urbanisation is the major driver of global land cover change, with 68% of the world's population projected to live in cities by 2050 (UN, 2018). Rapid population growth is causing natural elements within cities to be replaced by structural elements, leading to the destruction of rural character and the emergence of a concept called urban climate (Oke et al., 2017), which differs from rural environments.

Cities tend to have higher temperatures compared to surrounding rural areas. Impervious surfaces like asphalt and concrete absorb solar energy, increasing LST due to reduced vegetation and evapotranspiration, lower albedo, and increased anthropogenic urban heat. This phenomenon is known as the urban heat island (UHI) effect (Landsberg, 1981). Studies constantly show a positive correlation between LST and urbanisation. Some spectral indices like the normalised difference vegetation index (NDVI), normalised difference water index (NDWI), and normalised difference built-up area index (NDBI) are widely used to analyse the relationship between LST and LULC. NDVI is an index used to estimate vegetation cover based on the reflectance properties of leaves at red (Red) and near-IR (NIR) wavelengths. A region with a higher NDVI value has a lower LST. NDBI is obtained using the mid-infrared (MIR) and near-infrared (NIR) bands used to measure changes in urban landscapes; which have a positive relationship with LST (Shu et al., 2024).

The main reason for LU/LC changes is increased migration to cities in line with the socio-economic policies (Xie et al., 2023) and the growth of the service sector and industry, especially in developing countries. In Türkiye, rural-urban migration accelerated after the 1950s with rapid urban sprawl in coastal cities following the increase of tourism 1980s (Çınar et al., 2024). Antalya is important in Türkiye for tourism and agriculture – contributes 75% of the country – has experienced significant LULC changes, transforming natural and agricultural areas into urban infrastructure, contributing to rising temperatures (Atik et al., 2021).

This research offers a novel approach by integrating long-term Landsat satellite data with UHI analysis, tracking the spatial and temporal dynamics of urban expansion and LST changes across multiple decades. Unlike previous studies that often rely on short-term data, this research utilises the historical continuity of Landsat imagery to provide a comprehensive view of urban morphology and its environmental impacts. Focusing on Antalya, a rapidly urbanising Mediterranean city shaped by tourism and population growth, the research provides a localised, in-depth analysis of how diverse land uses – including urban, agricultural, and forested areas – affects LST and UHI patterns. Combining remote sensing with detailed land use classification contributes valuable insights into urbanisation's impact on regional climates. This research examines the effects of LULC change on urban temperatures (LST) between 1984 and 2022 in Antalya. It is aimed to determine;

1 LU/LC and LST in the city

2 NDVI and LST relationship

3 NDBI and LST relationship.

The result of the research will provide information on effective land use, where a balance is established between sustainable urban land use and climate change.

2 Materials and methods

2.1 Research area

Antalya is a typical coastal city of the Mediterranean region city located in south-western Türkiye (Figure 1). Antalya is located on a travertine terrain at an elevation of 47 meters. One of the hottest cities in the country, the city has a mild Mediterranean climate with hot and dry summers and rainy winters. The average temperature of the city, which is sunny 300 days a year, the average temperature typically ranges from 0°C to 36°C in July and August often exceeding 30°C. The coldest month on average is January, while the hottest month is July. Most of the annual precipitation 224 mm occurs in winter (December-January-February) and partly in spring and fall (March-April-November). Rainfall is very low in the season between May and October. The annual average number of days with total daily precipitation of 50 mm or more is 2.21 (MGM, 2021).

Figure 1 Location map of Antalya City with boundaries and research area (see online version for colours)

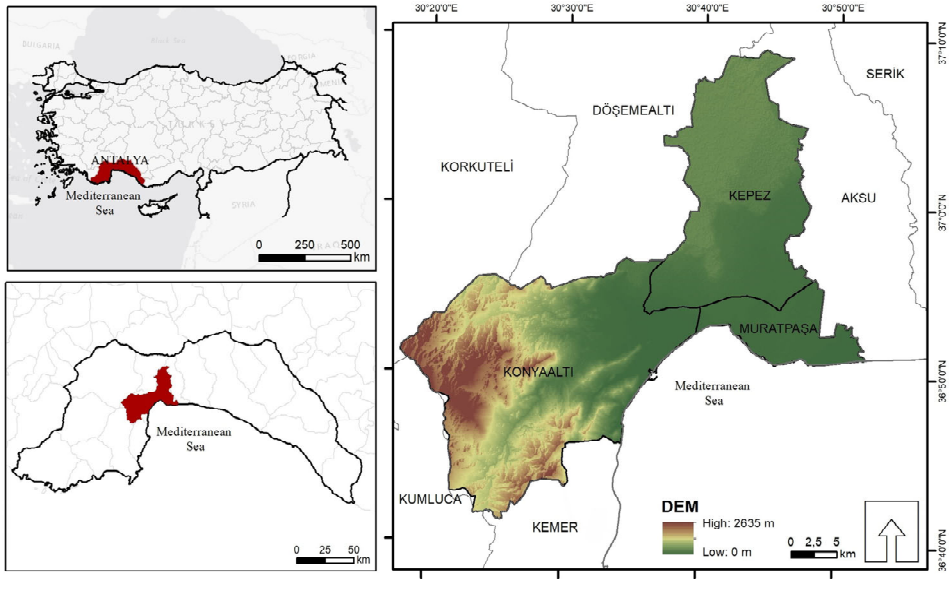

The landscape of the city consists of cliffs, beaches, forests, natural bushes, orchards, urban areas, agricultural lands, and water elements. The entire research area is 138,000 hectares. Antalya is a rapidly growing city with a population of 2.5 million. The research area covers Konyaaltı, Muratpaşa, and Kepez districts within the city boundaries. The provincial population in 2022 was 2,688,004 and the population of these three central districts is approximately 1,339,763 (TÜİK, 2022).

2.2 Satellite data used and processing

In this research, LU/LC and LST maps were created using Landsat satellite images. The main material of the research consists of satellite images from 1984, 2003, and 2022. These images were downloaded free of charge from the US Geological Survey (USGS) portal (http://earthexplorer.usgs.gov/) in GeoTIFF format and georeferenced using the World Geodetic System (WGS) 1984 coordinate reference system. Atmospheric conditions and seasonal effects were considered in the selection of satellite images, with a preference for cloudless images to ensure accurate analysis. The spatial data georeferenced according to the research area were processed using Esri ArcGIS and ArcMap software, while tables were organised using Microsoft Excel.

2.3 Land use/land cover

The LU/LC maps determined by the controlled classification method were prepared separately for the years 1984, 2003, and 2022 and were classified into four classes relevant to the research scope. The classes defined in the context are:

1 artificial surfaces

2 agricultural lands

3 natural and semi-natural areas

4 water surfaces.

Training data were collected based on the defined classes. The accuracy of the controlled classification results was calculated using an error matrix created separately for each year, based on 517 control points.

2.4 Calculation of urbanisation indicators; NDVI and NDBI

Landsat 5 TM (dated 19.07.1984 and 05.07.2003), and Landsat 8 OLI-TIRS (dated 18.07.2022) satellite images taken in July were obtained. Band 6 and Band 10 were used. Satellite images were cropped and georeferenced according to the research area boundaries and NDVI vegetation cover ratio [equation (1)], and NDBI settlement areas ratio [equation (2)] and LST [equations (3)–(8)] were calculated for the districts within the research area (Li et al., 2024; Kumar et al., 2023).

$$\mathrm{NDVI} = (\mathrm{NIR} - \mathrm{Red})/(\mathrm{NIR} + \mathrm{Red}) \tag{1}$$

$$\mathrm{NDBI} = (\mathrm{MIR} - \mathrm{NIR})/(\mathrm{MIR} + \mathrm{NIR}) \tag{2}$$

2.5 Land surface temperature

The LST was generated using the Mono-Window Algorithm (Srivastava, 2020) from the geometrically and radiometrically corrected Landsat satellite images from 1984, 2003, and 2022, Band 6 for Landsat 5 and Band 10 for Landsat 8. The following sequence of operations was applied to calculate surface temperatures from the thermal bands. From Landsat 5 TM, only the first two steps were needed [equation (3)–equation (4)].

First, atmospheric spectral radiance was calculated from the thermal image band values of Landsat images using the parameters in the metadata file of the satellite image [equation (3)] (Sobrino et al., 2004).

$$L_\lambda = L_{MIN} + (L_{MAX} - L_{MIN}) * DN / 255 \tag{3}$$

L_λ represents the spectral radiance (from satellite metadata) or top of atmospheric (TOA) radiance and DN thermal band reflectance values. For Landsat 5, L_{MIN} = 1.238 and L_{MAX} = 15.30; for Landsat 8, L_{MIN} = 0.10033 and L_{MAX} = 22.00180

In the second step, after the reflectance values were converted to brightness values, they were converted to spectral brightness temperature using thermal constants provided from the metadata file of the thermal band data, and Kelvin conversion was performed (Fahmy et al., 2023).

$$BT = \left(K_2 / \mathrm{Ln}\left(K_1 / L_\lambda\right) + 1\right) - 273.15 \tag{4}$$

K_1 and K_2 define the conversion constants for the thermal band in the satellite metadata. For Landsat 5 K_1 = 607.76 and K_2 = 1,260.56, for Landsat 8 K_1 = 774.8853 and K_2 = 1,321.0789 (Band 10).

Then, the vegetation cover ratio is determined using the NDVI plant and soil values of the research area. This ratio is determined by using the maximum ($NDVI_{max}$) and minimum ($NDVI_{min}$) values over NDVI (Sobrino et al., 2004).

$$P_V = \left[(NDVI - NDVI_{min}) / (NDVI_{max} - NDVI_{min})\right]^2 \tag{5}$$

Irradiance value is an important parameter used in the calculation of ground surface temperatures. In this research, the method based on NDVI values was used. In this method, NDVI values were threshold as soil and plant values, and the diffusivity values of the research area were calculated (Fahmy et al., 2023).

$$\varepsilon = 0.004\,Pv + 0.986 \tag{6}$$

In the last step, the values in formulas (4) and (6) were used to calculate the surface temperature. Here, BT is the temperature value calculated in the previous steps, λ is the average wavelength of the thermal tape used (10.9 μm) and ε is the emissivity value. The value of ρ is constant and is calculated using the following formula [equation (8)]. Band 10 was used for Landsat 8 and Band 6 for Landsat 5 (Fahmy et al., 2023).

$$LST = BT / 1 + (\lambda) * (BT / \rho) * \ln(\varepsilon) \tag{7}$$

$$\rho = h * c/\sigma = 1.438 \times 10^{-2}\,mK \tag{8}$$

h is Planck's constant (6.626 * 10^{-34} Js), σ: Boltzmann constant (1.38 * 10^{-23} J/K), c is the speed of light (2.998 * 10^8 m/s).

Finally, formula (9) was used to calculate the UHI effect. μ represents the average LST value and σ represents the standard deviation of LST.

$$UHI = \mu + \frac{\sigma}{2} \tag{9}$$

Areas with UHI and non-UHI were identified through the calculation of LST and UHI values with equations (7) and (9). Areas where the LST > UHI was classified as heat

island areas, while those 0< LST ≤ UHI were classified as non-UHI areas (Guha et al., 2018). The results show the hottest part of the city.

Since it is not appropriate to directly compare the LST variability in thermal images of Landsat data from different years, standardisation was performed using formula (10), and the variables were made proportional to each other (Ullah et al., 2019).

$$LST_s = LST - LST_u / LST_\Omega \quad (10)$$

LST_s = standardised LST, LST_u = mean of estimated LST from 1984 to 2022, LST_Ω = Standard deviation of LST from 1984 to 2022.

To find the proportional area covered by areas with different surface temperatures, surface temperature values were classified into five ranges: <25, 25–30, 30–35, 35–40, and >40°C. The purpose of the classification is to evaluate the change of temperature values in different areas over the years.

3 Results and discussion

3.1 Results

3.1.1 Land use/land cover change 1984 to 2022

The research reveals the changes of urban sprawl on LU/LC for the city of Antalya for the period 1984–2022. Figure 2 represents the map of historical data in LU/LC classes generated from Landsat imagery. The LU/LC classification maps for Kepez, Konyaaltı, and Muratpaşa districts in Antalya were calculated using 517 reference points, achieving accuracies of 91% for 1984, 90% for 2003, and 91% for 2022. In 1984, urban areas were mainly in the south-north direction, with agricultural lands in the northeast and natural/ semi-natural areas in the southwest.

Table 1 1984, 2003 and 2022 land uses (km²)

LU/LC		*1984 (km²)*	*(%)*	*2003 (km²)*	*(%)*	*2022 (km²)*	*(%)*	*Net change (%)*
1	Artificial surfaces	55.584	6.17	99.494	11.04	154.230	17.12	177
2	Agricultural areas	279.364	30.99	219.765	24.39	69.118	7.67	-75
3	Natural and semi-natural areas	553.892	61.47	571.254	63.40	671.489	74.53	21
4	Water surfaces	12.176	1.35	10.503	1.17	6.179	0.69	-49
Total		901.016	100	901.016	100	901.016	100	

Table 2 Area change between 1984–2022

LU/LC			*LU/LC*	*Area change (km²)*	*%*
1	Artificial surfaces	2	Agricultural areas	3.13	0.96
		3	Natural and semi-natural areas	4.54	1.39
2	Agricultural areas	1	Artificial surfaces	61.37	18.74
		3	Natural and semi-natural areas	179.95	54.93
		4	Water surfaces	0.27	0.08

Table 2 Area change between 1984–2022 (continued)

LU/LC			*LU/LC*	*Area change (km²)*	*%*
3	Natural and semi-natural areas	1	Artificial surfaces	43.53	13.29
		2	Agricultural areas	27.44	8.38
		4	Water surfaces	0.53	0.16
4	Water surfaces	1	Artificial surfaces	1.41	0.43
		2	Agricultural areas	0.78	0.24
		3	Natural and semi-natural areas	4.60	1.41

Figure 2 Land use/land cover categories and distributions of 1984, 2003 and 2022 (see online version for colours)

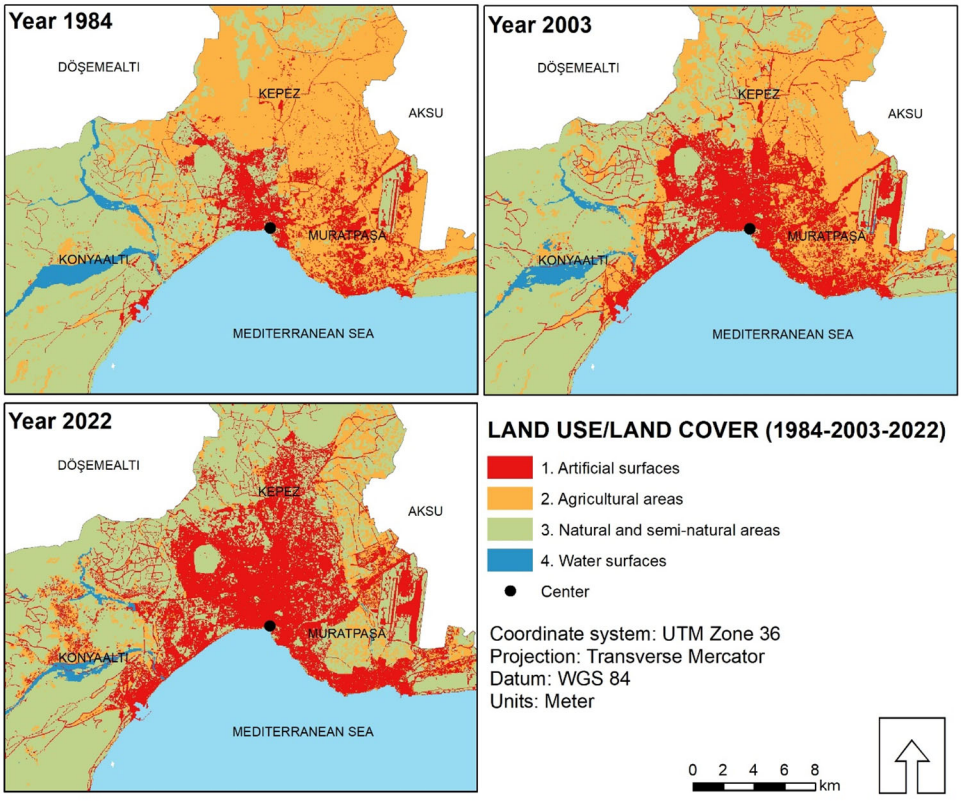

Urban areas expanded from 55.584 km² in 1984 to 99.494 km² in 2003 and 154.230 km² in 2022 (Table 1). In 1984, urban areas covered 6.17% of the total land area, and by 2022, this increased 17.12% (Figure 2). The results show that in the last 28 years, 61.38% of agricultural areas and 43.53% of natural and semi-natural areas have been transformed into artificial surfaces (Table 2). This result coincides with the research conducted by Tekkanat (2018) for the centre of Antalya between 2000 and 2012. In Muratpaşa, mixed agricultural areas became urban areas, while in Konyaaltı, natural areas were converted to

various recreational areas, and mixed agricultural areas turned into discontinuous residential areas.

The LU/LC shows a main trend of gradually increasing residential areas and decreasing agricultural lands in the research. Period from 1984 to 2022, unplanned and rapid urban sprawl expanded east, west, and north of the city, reducing agricultural and natural lands while increasing built-up land cover. This rapid urbanisation has resulted in the transformation of LST and SUHI and adverse city climate.

Figure 3 Spatial variations of land surface temperature 1984 to 2022 (see online version for colours)

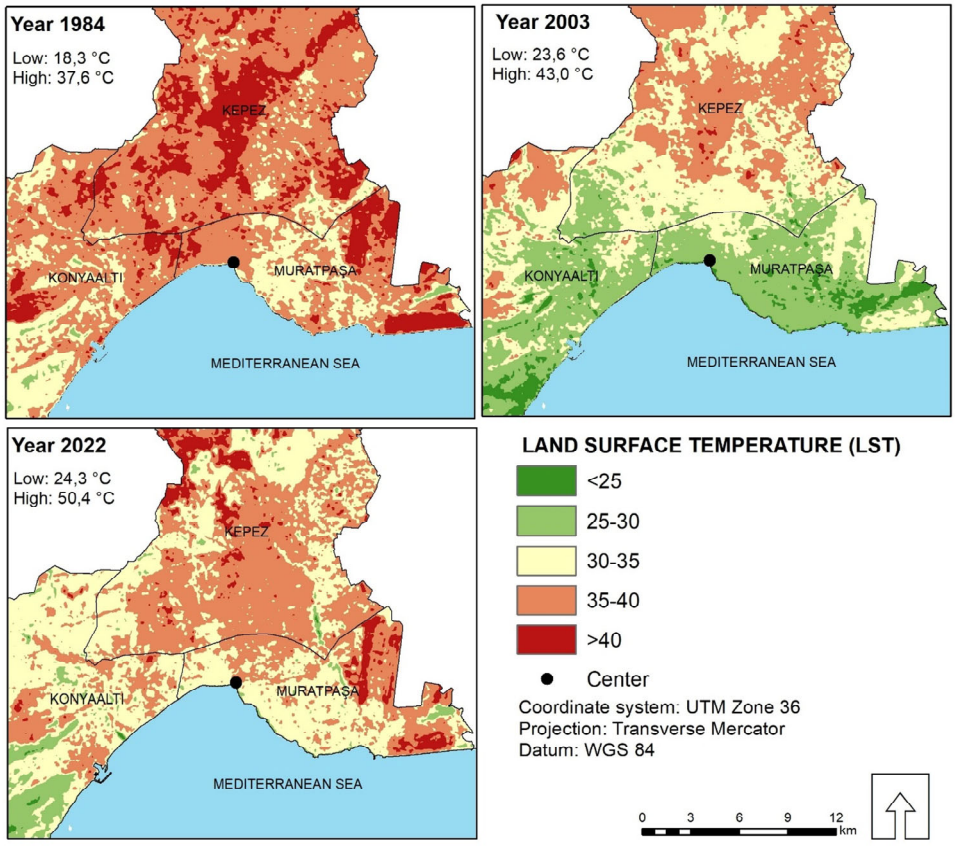

3.1.2 Land surface temperature change 1984 to 2022

The historical results of LST changes (1984–2022) derived from Landsat thermal bands (described in section 2.5) are presented in Figure 3, which illustrates the LST distribution of Antalya city. The colours in the figure, ranging from green to red, represent low to high temperatures. This research found that from 1984 to 2022, LST increased in all classes due to urban area expansion, exacerbated by global warming and climate change. Over the 28 years, the maximum surface temperature increased from 37.7°C in 1984 to 50.5°C in 2022 (Table 3).

Antalya's urban growth is the result of both planned and unplanned political decisions with settlement concentrated in the north and urban sprawl extending east and north-west of Antalya. Rapid urban development between 1984 and 2022, most of the agricultural land transformed into urban areas or bare land, causing significant changes in LST. The minimum temperature increased by 5.9°C and 6.28°C and the maximum temperature increased by 5.3°C and 12.8°C in 2003 and 2022, respectively. This increase in LST indicates that the conversion of natural areas and agricultural lands into urban areas, along with rising population density, has accelerated surface temperature increases. SUHI zones are mostly concentrated in the Airport area in Muratpaşa and the densely built-up Kepez region.

Table 3 Average land surface temperature changes in the research area between 1984 and 2022

Mean LST	*1984 (°C)*	*2003 (°C)*	*2022 (°C)*
T_{min}	6.82	12.8	13.1
T_{max}	37.7	43	50.5
T_{mean}	26.9	30.3	31.7

The proportional coverage of areas with different surface temperatures is detailed in Table 4, indicating the lowest temperature as 6.8°C, and the highest as 50°C, with temperatures above 40°C covering about 16% of the total area in 2022. There are no recorded areas above 40°C from 1984 to 2003. Additionally, areas with a surface temperature of 35–40°C, absent in 1984, increased after 2003, while areas below 25°C decreased.

Table 4 Land surface temperature regions of Antalya City for the years 1984–2022

LST zones classes (°C)	*1984 area (km^2)*	*(%)*	*2003 area (km^2)*	*(%)*	*2022 area (km^2)*	*(%)*
<25	115.549	12.85	58.02	6.45	82.247	9.15
25–30	498.074	55.40	412.102	45.84	191.73	21.32
30–35	248.287	27.62	251.696	27.99	239.336	26.62
35–40	0.00	0.00	174.912	19.45	242.325	26.95
>40	0.00	0.00	0.00	0.00	143.45	15.96

3.1.3 Relationship between urban indices and LST

Spectral indices like NDVI and NDBI strongly correlate with LST, highlighting the impact of built-up areas in raising temperature. NDBI and LST have a positive relationship, while NDVI shows a negative relationship. The correlation tests performed in this research also yielded significant results ($p < 0.005$). The correlation coefficient (R^2) indicated a strong relationship between LST and both NDVI and NDBI for each research year (Figure 4).

Figure 4 Correlation between land surface temperature and land use/land cover indices (see online version for colours)

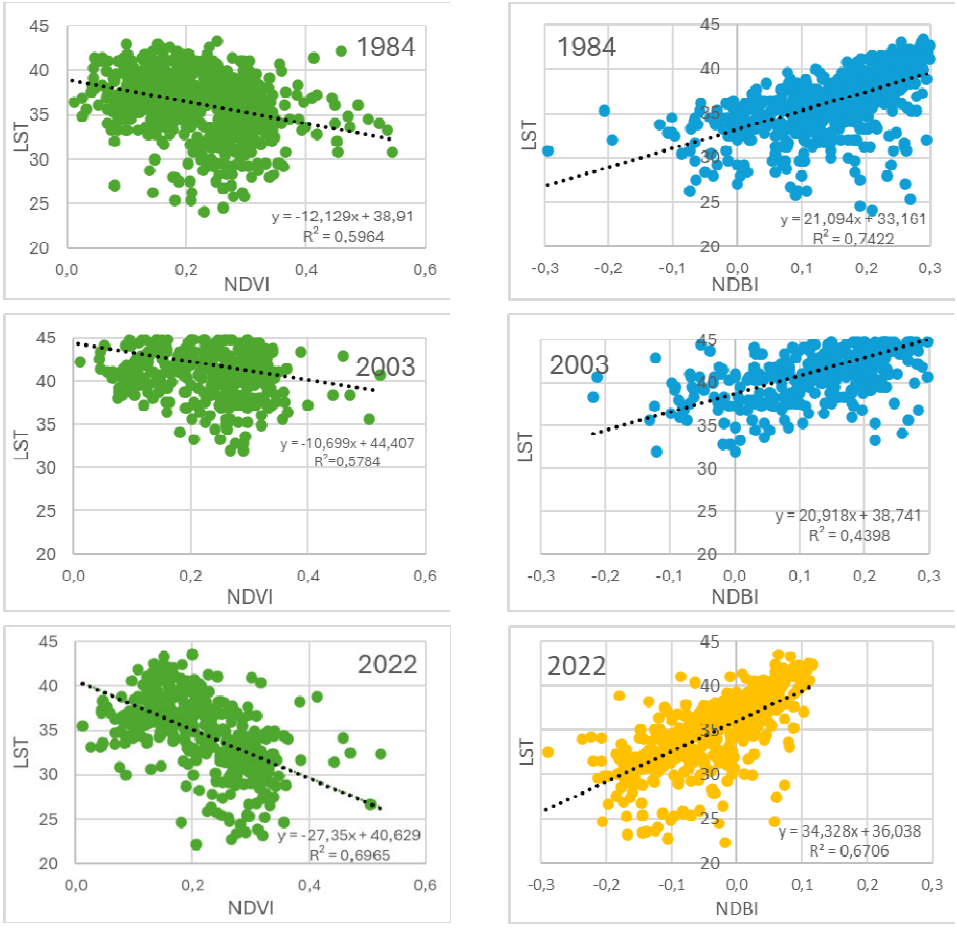

To determine LST by land cover, changes in NDVI (Figure 5) and NDBI (Figure 6), as urbanisation indicators, were analysed. Accordingly, it was determined that forested areas with high NDVI values, especially in Muratpaşa district and north of Kepez district, decreased and urban areas increased. Forested areas in Konyaaltı district did not undergo any change due to being protected areas. Again, agricultural areas with medium NDVI values concentrated in Kepez and Muratpaşa districts faced urbanisation in 2003 and 2022 and had high NDBI values. Areas with high NDBI values are mainly concentrated in the southern part of the research area extending toward the north and northeast.

Figure 5 Spatial variations of NDVI 1984 to 2022 (see online version for colours)

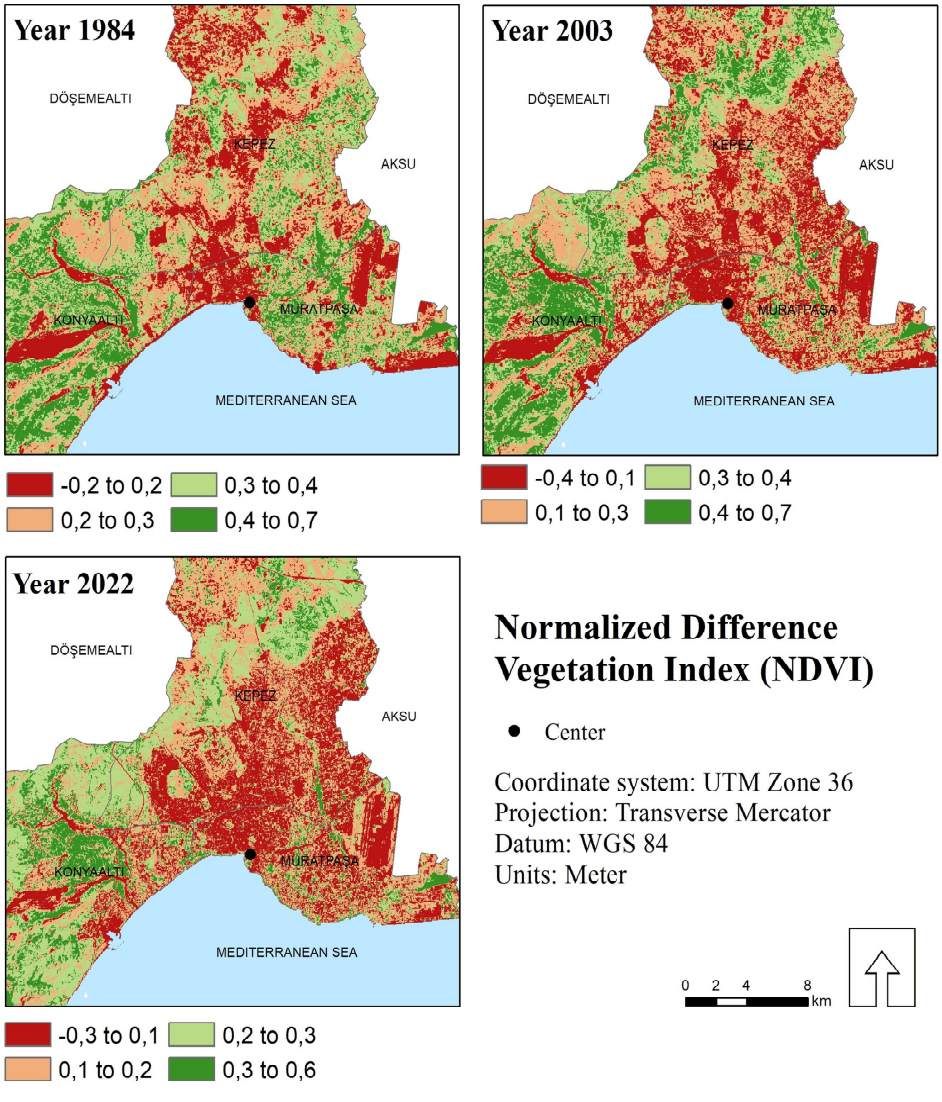

Figure 7 shows the temporal surface temperature variation of the land cover classes of the research area. Urban areas have the highest LST and SUHI formation, while agricultural lands and natural areas have lower LST values. In 1984, urban areas had a surface temperature of about 30°C, while in 2022 it was 35.28°C. Green areas had LST values around 6°C lower than urban areas. These findings are consistent with many studies that have examined LU/LC classes and their effects on LST. The research showed that as vegetation is replaced by built-up structures in urban areas LST values rise. LST

increased not only in structural areas but also in vegetated areas from 1984 to 2022. Urban sprawl increases LST values even in green areas as a phenomenon that triggers global temperatures. Although vegetation is known to mitigate the SUHI effect in cities (Ribeiro et. al., 2024) rapid urbanisation still leads to higher LST values in green areas within the city.

Figure 6 Spatial variations of NDBI 1984 to 2022 (see online version for colours)

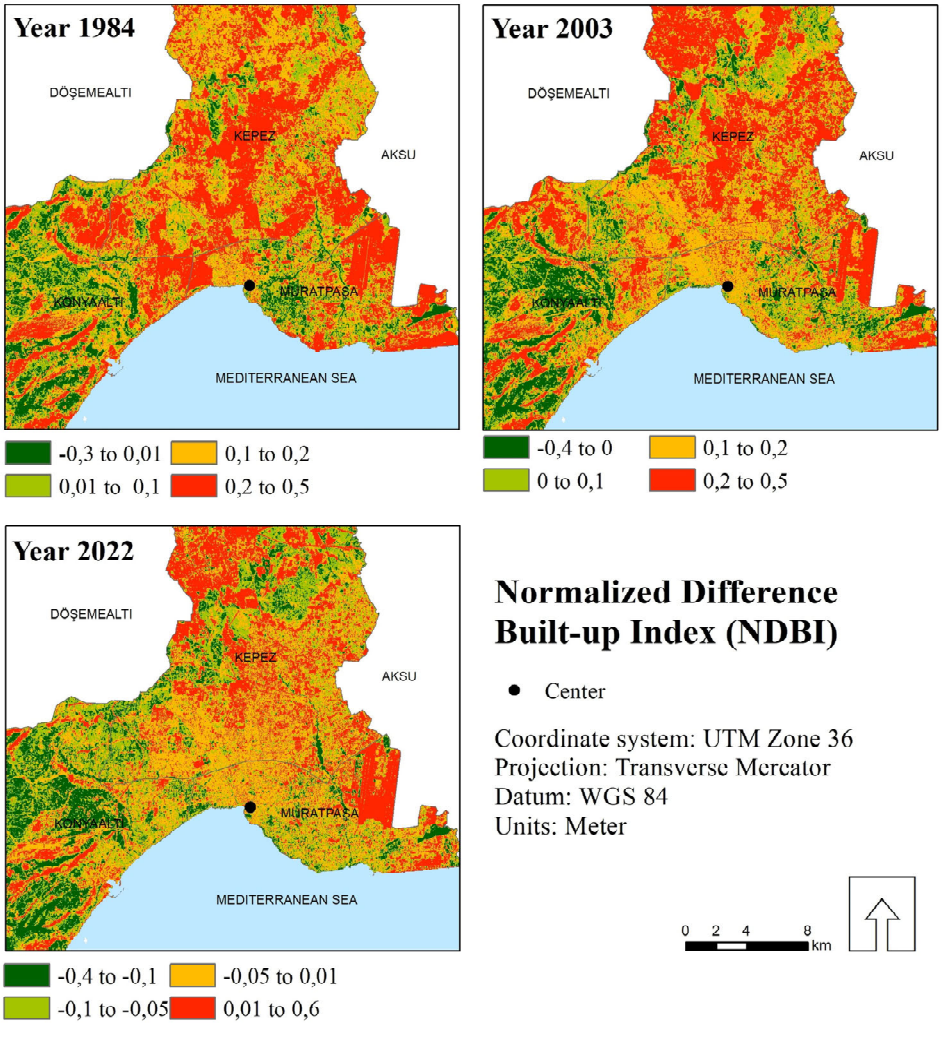

Figure 7 Yearly variation of land surface temperature mean of different land use/land cover classes in the research area (see online version for colours)

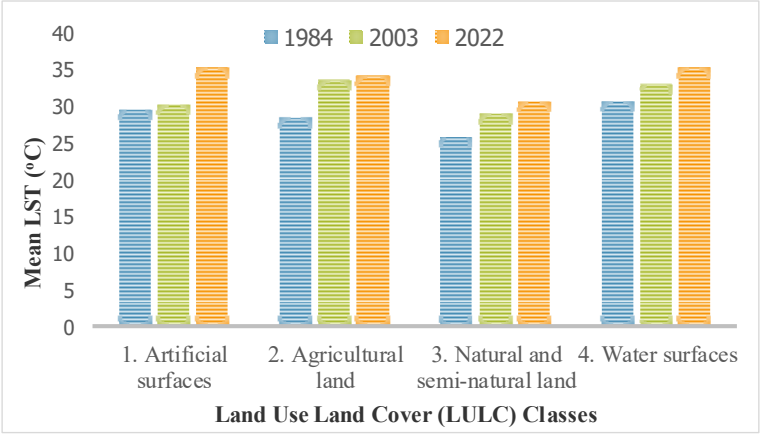

3.1.4 UHI and Non-UHI zones

Since Antalya is a coastal city, it shows a positive UHI effect in both summer and winter. The research results show that while the UHI effect remains consistent from 1984–2022, the overall temperature values have gradually increased. The south-north vertical axis of the area exhibits the highest density of UHI zones. In 1984, the UHI zones had a temperature of 29.1°C, 32.54°C by 2003, which increased to 34.33°C by 2022. The increase in UHI temperatures over time increased by approximately 3°C during the period of the fastest land change and by 1°C in the following period. Although the spatial extent of UHI zones has remained consistent throughout the research period. Their intensity has grown in the city centre due to the expansion of residential areas and a corresponding decrease in vegetation cover. As a result, UHI is most intense in the city centre. The UHI temperature in Antalya increased by 5.2°C between 1984 and 2022.

3.2 Discussion

3.2.1 Consequences of urbanisation

Urban sprawl resulting from population growth increases pressure on natural areas, leading to changes in LU/LC characteristics and high LST values (Agdas and Yenen 2023; Hasnat, 2022). The expansion of residential areas at the expense of agricultural land is a common trend and these areas have high LST values, leading to the formation of UHI. Therefore, observing this change in land cover is important for understanding regional climate.

In the past decade, the impact of UHI has been examined from multiple perspectives. For example, many studies have investigated the distribution patterns of UHI and the relationship between air temperature-land surface temperature and land cover/land use (Srivastava, 2020; Lin et al., 2023) and ecosystem services. Climate studies conducted at various scales have identified topography, population size, urban geometry, canyon geometry, urban surface characteristics, land use pattern, agricultural area ratio, and

green area ratio as the most significant factors influencing UHI density (Al-Marzooqi et al., 2021; Yu et al., 2020).

It is known that many cities around the world are facing problems related to global warming and Antalya, one of the most important cities in Türkiye, is also facing climatic challenges. The findings of this research indicate there is a strong urbanisation trend in Antalya, with related land cover changes particularly concentrated in natural and agricultural areas. Since 1984, the increase in the urban area has contributed to the rise in employment opportunities and the influx of urban population due to the opening of the city to tourism as a result of the Tourism Incentive Law No. 2634 enacted in the 1980s. Significant investments in the tourism sector have led to a period of increased commercial activities and unplanned urbanisation. This finding aligns with other studies (Akış, 2012), which also report that economic policies have driven urban growth and the conversion of agricultural lands into urban uses in Antalya. Although this situation is important for economic development, it causes unplanned urbanisation. The transformation of agricultural lands and natural areas into artificial surfaces because of this rapid urban sprawl has also harmed the urban environment and climate.

This research found that urban areas in Antalya increased by 177% from 1984 to 2022, while agricultural and natural areas decreased by 75% and 21%, respectively. The city has a structure where activities based on housing, industry, agriculture, and tourism are intensive. Most of the natural areas and forests of the research area are within the boundaries of the Olympos Beydağları National Park, which is the natural border to the west. There are urban forests and agricultural areas in the north and east of the area. The central part where residential areas are concentrated causes the average LST value to increase and SUHI to occur. These findings are like many studies examining LU/LC classes and their effects on LST (Jia et al., 2022; Ibrahim et al., 2021; Pan et al., 2021), which indicate that urban sprawl increases LST values even in vegetated areas phenomenon triggering global temperatures.

3.2.2 Spatial patterns of LST

Türkiye's Mediterranean coastal cities have entered an aggressive urbanisation process as a result of rapid developments in tourism (Atik et al., 2021). The urban sprawl and economic development of Antalya have also taken place at the expense of the development of the tourism sector of natural areas and fertile agricultural lands. This led to an increase in average LST values in general. When the surface temperature results are examined, it is seen that there are significant differences between the surface temperature of the large green area covered in the west of the city and the surface temperature of the city centre. In the research conducted according to surface temperatures, Antalya city centre and its surroundings are in the temperature range of 33ºC–45ºC, while the temperature range is mostly between 30ºC–35ºC in the agricultural areas in Kepez district in the northeast of the area. Antalya Airport, located in the east of the city, and Lara Dunes, administratively located in Muratpaşa district, are among the regions with the highest temperature reflection in the temperature range of 38ºC–50ºC. Jia et al. (2022) also concluded in their research of Jiaozuo City, China that the urban sprawl is the main driving force to rise the LST in the city centre.

In this research, land use classes were determined using NDVI and NDBI techniques to see the effects of different land uses on surface temperatures. Guha et al. (2018) also investigated the built-up areas among have higher LST values as compared to vegetated

areas. Accordingly, urban surface temperatures, although green areas in less densely urbanised areas have more vegetation and higher NDVI values than built-up areas, the LST difference is lower than in the urbanised area. This is due to the high proportion of vegetation and low proportion of built-up land within and between the green areas. In the future, the dynamics of urbanisation is a topic that needs to be investigated.

The purpose of land use planning is to ensure the balance between conversation and use to manage the land effectively and sustainability. Currently, the government and local governments for the city of Antalya have focused on the development of urban green areas to mitigate climate change. Studies conducted on a local scale have shown that green spaces in the city can have a positive effect on the reduction of LST and the formation of SUHI pockets. In these studies, conducted in cities, it was determined that the increase in vegetation density and albedo height decreased the LST effect. Accordingly, it shows that urban forests are more effective in reducing urban temperatures than grasslands (Yu et al., 2020).

Satellite imagery is both an economical and easy-to-access resource for assessing temporal and spatial SUHI changes over a large region. The resolution of the Landsat satellite imagery used in this research (30 metres) has limitations in capturing fine detail, especially in heterogeneous urban areas. The use of higher-resolution satellite data may allow a more detailed examination of urban sprawl and land surface temperature changes. However, Landsat was preferred because of its advantage in providing long-term data. In addition, surface temperature classifications were based on general thresholds, but these thresholds may vary depending on local environmental conditions. Although our research achieved high accuracy in land use and land cover classifications, the lack of field validation data is another limitation. Future studies supporting remote sensing results with field data will increase the accuracy of the results. Finally, although our research considered socio-economic factors in a broad sense, it did not analyse these factors quantitatively. The inclusion of these factors in future research will contribute to a more comprehensive understanding of urban growth and its impacts. In addition, the use of more urban indices such as NDMI and NDWI will expand the range of results and enable more specific recommendations to be developed. The evaluation of LST values together with other city-specific climatic data can help urban planners and politicians make the right decisions.

4 Conclusions

This study investigates the effects of urban pattern change on the urban climate in Antalya. In this way, LU/LC and LST maps were produced for Antalya, a coastal city, using Landsat satellite images and evaluated from 1984 to 2022. The main conclusions of the research;

1 The expansion of urban areas in Antalya in the period 1984–2022 has led to a significant decrease in agricultural and natural areas.

2 The urban area increased from 55.584 km² in 1984 to 154,230 km² in 2022. During the research period, urban areas increased from 6% to 17%.

3 61.38% of agricultural lands and 43.53% of natural/semi-natural areas have been transformed into artificial surfaces.

4 The LST increased from 37.7ºC in 1984 to 50.5ºC in 2022. That is linked to the expansion of urban areas and climate change.

5 Min. temperature increased by 5.9ºC and max. Temperature increased by 12.8ºC at surface temperatures.

6 Antalya's UHI effect has been observed in both summer and winter. UHI temperature increasing from 29.1ºC in 1984 to 34.33ºC in 2022. The density of UHI zones has increased with the expansion of urban areas and the decrease in vegetation especially in the city centre.

7 Spectral indices NDVI (negative relationship) and NDBI (positive relationship) results for Antalya have a strong relationship with LST. These findings show that LST increases with the expansion of urban areas.

8 While the average surface temperature of urban areas was 30ºC in 1984, increased to 35.28ºC in 2022.

9 Green areas have a surface temperature of about 6ºC lower than urban areas, but rapid urban sprawl also increases LST in these areas.

Sustainable urban land use development and urban greenery are the most important priorities to mitigate the SUHI effect in cities. However, it is crucial to preserve and expand the city's green spaces, particularly in densely populated areas, which show 1–2ºC higher LST. Achieving sustainable land use development needs long-term planning and integrated policies.

References

Agdas, M.G. and Yenen, Z. (2023) 'Determining land use/land cover (LULC) changes using remote sensing method in Lüleburgaz and LULC change's impacts on SDGs', *European Journal of Sustainable Development*, Vol. 12, No. 1, p.1.

Akış, A. (2012) 'Turizmin Kentsel Gelişim Üzerine Etkileri: Bir Örnek İnceleme Antalya-Türkiye', *Doğu Coğrafya Dergisi*, Vol. 16, No. 25, pp.193–206.

Al-Marzooqi, M., Bilal, H., Govindan, R. et al. (2021) 'Impact of the urban heat island effect on the climate of the State of Qatar', *International Journal of Global Warming*, Vol. 24, Nos. 3/4, pp.400–419.

Atik, M., Ortaçeşme, V. and Yıldırım, E. (2021) 'Anticipating an urban green infrastructure design for the Turkish Mediterranean City of Antalya', in Catalano, C., Andreucci, M.B., Guarino, R., Bretzel, F., Leone, M., Pasta, S. (Eds.): *Urban Services to Ecosystems. Future City*, Vol. 17, pp.243–263, Switzerland, Springer Cham.

Çinar, I., Ardahanlıoğlu, Z.R. and Toy, S. (2024) 'Land use/land cover changes in a Mediterranean summer tourism destination in Turkey', *Sustainability*, Vol. 16, No. 14, p.1480.

Fahmy, A.H., Abdelfatah, M.A. and El-Fiky, G. (2023) 'Investigating land use land cover changes and their effects on land surface temperature and urban heat islands in Sharqiyah Governorate, Egypt', *The Egyptian Journal of Remote Sensing and Space Sciences*, Vol. 26, No. 2023, pp.293–306.

Guha, S., Govil, H., Dey, A. nad Gill, N. (2018) 'Analytical study of land surface temperature with NDVI and NDBI using Landsat 8 OLI and TIRS Data in Florence and Naples City, Italy', *European Journal of Remote Sensing*, Vol. 51, No. 1, pp.667–678.

Hasnat, G.N.T. (2022) 'Assessment of spatiotemporal distribution pattern of land surface temperature with incessant urban sprawl over Khulna and Rajshahi City Corporations', *Environmental Challenges*, Vol. 9, No. 2022, p.100644.

Humbal, A., Chaudhary, N. and Pathak, B. (2023) 'Urbanization trends, climate change, and environmental sustainability', in Pathak, B. and Dubey, R.S. (Eds.): *Climate Change and Urban Environment Sustainability. Disaster Resilience and Green Growth*, pp.151–166, Springer, Singapore.

Ibrahim, M., Koch, B. and Datta, P. (2021) 'Evaluate the effect of land surface temperature in arid and semi-arid lands using potential remote sensing data and GIS techniques', *International Journal of Global Warming*, Vol. 24, Nos. 3/4, pp.342–355.

Jia, X., Song, P., Yun, G., Li, A., Wang, K., Zhang, K. and Ge, S. (2022) 'Effect of landscape structure on land surface temperature in different essential urban land use categories: a case study in Jiaozuo, China', *Land*, Vol. 11, No. 10, p.1687.

Kumar, B.P., Anusha, B.N., Babu, K.R. and Sree, P.P. (2023) 'Identification of climate change impact and thermal comfort zones in semi-arid regions of AP, India using LST and NDBI techniques', *Journal of Cleaner Production*, Vol. 407, No. 15, p.137175.

Landsberg, H.E. (1981) 'The urban climate', in Van Mıeghem, J., Hales, A.L. and Donn, W.L. (Eds.): *International Geophysic Series*, Vol. 28.

Li, X., Xu, J., Jia, Y., Liu, S., Jiang, Y., Yuan, Z., Du, H., Han, R. and Ye, Y. (2024) 'Spatio-temporal dynamics of vegetation over cloudy areas in Southwest China retrieved from four NDVI products', *Ecological Informatics*, Vol. 81, No. 2024, p.102630.

Lin, J., Qiu, S., Tan, X. and Zhuang, Y. (2023) 'Measuring the relationship between morphological spatial patterns of green space and urban heat islands using machine learning methods', *Building and Environment*, Vol. 228, No. 2022, p.109910.

Meteoroloji Genel Müdürlüğü (MGM) (2021) *Antalya Climate Data* [online] https://https://www.mgm.gov.tr/?il=Antalya (accessed 8 December 2022).

Oke, T.R., Mills, G., Christen, A. and Voogt, J.A. (2017) *Urban Climates*, Cambridge University Press, Cambridge.

Pan, Y., Gao, Y. and Li, S. (2021) 'Impacts of land use/land cover distributions and vegetation amount on land surface temperature simulation in East China', *Earth and Space Science*, Vol. 8, No. 5, pp.1–17.

Ribeiro, M.P., Menezes, g.P., Figueiredo, G.K.D.A., Mello, K. and Valente, R.A. (2024) 'Impacts of urban landscape pattern changes on land surface temperature in Southeast Brazil', *Remote Sensing Applications: Society and Environment*, Vol. 33, No. 2024, p.101142.

Shu, B., Chen, Y., Zhang, K., Dehghanifarsani, L. and Beni, M.A. (2024) 'Urban engineering insights: Spatiotemporal analysis of land surface temperature and land use in urban landscape', *Alexandria Engineering Journal*, Vol. 92, No. 2024, pp.273–282.

Sobrino, J.A., Jiménez-Muñoz, J.C. and Paolini, L. (2004) 'Land surface temperature retrieval from LANDSAT TM 5', *Remote Sensing of Environment*, Vol. 90, No. 2004, pp.434–440.

Srivastava, M.R. (2020) 'Urban heat island effect over Delhi NCR using LANDSAT™ data', *International Journal of Global Warming*, Vol. 22, No. 3, pp.272–294.

Tekkanat, İ.S. (2018) 'Antalya İl Merkezi'nin CORINE Sınıflandırmasına Göre Arazi Örtüsü/Kullanımındaki Değişimlerin Değerlendirilmesi', in *Proceedings of the Uluslararası Antalya Kongresi*, Antalya, Türkiye, 1–3 March.

TÜİK (2022) [online] https://www.tuik.gov.tr/ (accessed 10 December 2022).

Ullah, S., Ahmad, K., Sajjad, R.U., Abbasi, A.M., Nazeer, A. and Tahir, A.A. (2019) 'Analysis and simulation of land cover changes and their impacts on land surface temperature in a lower Himalayan region', *Journal of Environmental Management*, Vol. 245, No. 2019, pp.348–357.

United Nations (UN) (2018) *United Nations World Urbanization Prospects: The 2018 Revision* [online] https://population.un.org/wup/Publications/Files/WUP2018-Report.pdf (accessed 10 January 2024).

Xie, Q., Han, Y., Zhang, L. and Han, Z. (2023) 'Dynamic evolution of land use/land cover and its socioeconomic driving forces in Wuhan, China', *International Journal of Environmental. Research and Public Health*, Vol. 20, No. 4, p.3316.

Yu, Z., Yang, G., Zuo, S., Jorgensen, G., Koga, M. and Vejre, H. (2020) 'Critical review on the cooling effect of urban blue-green space: a threshold-size perspective', *Urban Forestry & Urban Greening*, Vol. 49, p.126630.

Nomenclatures and abbreviations

	Definitions
BT	Brightness temperature
ε	Irradiance
λ	The average wavelength of the thermal tape
μ	the average LST value
σ	the standard deviation of LST
ρ	Constant
h	Planck's constant
σ	Boltzmann constant
c	speed of light
K	Kelvin conversion constants
L_λ	Spectral radiance
LU/LC	Land use/land change
NIR	Near Infrared
NDVI	Normalized difference vegetation index
NDBI	Normalized difference built-up area index
NDMI	Normalized difference moisture index
NDWI	Normalized difference water index
MIR	Mid-infrared
OLI	Operational land imager
Pv	Vegetation cover ratio
SUSHI	Surface urban heat island
TIRS	Thermal infrared
TM	Thematic mapper
T_{min}	Minimum temperature
T_{max}	Maximum temperature
UHI	Urban heat island
USGS	United States Geological Survey
WGS	World geodetic system